AGU PUBLICATIONS

Geophysical Research Letters

RESEARCH LETTER
10.1002/2016GL070404

Special Section:
First results from NASA's Magnetospheric Multiscale (MMS) Mission

# Observations of large-amplitude, parallel, electrostatic waves associated with the Kelvin-Helmholtz instability by the magnetospheric multiscale mission

**F. D. Wilder[1], R. E. Ergun[1,2], S. J. Schwartz[1,3], D. L. Newman[4], S. Eriksson[1], J. E. Stawarz[1,2], M. V. Goldman[4], K. A. Goodrich[1,2], D. J. Gershman[5], D. M. Malaspina[1], J. C. Holmes[1,2], A. P. Sturner[1,2], J. L. Burch[6], R. B. Torbert[7], P.-A. Lindqvist[8], G. T. Marklund[8], Y. Khotyaintsev[9], R. J. Strangeway[10], C. T. Russell[10], C. J. Pollock[5], B. L. Giles[5], J. C. Dorrelli[5], L. A. Avanov[5], W. R. Patterson[5], F. Plaschke[11], and W. Magnes[11]**

[1]Laboratory of Atmospheric and Space Physics, University of Colorado Boulder, Boulder, Colorado, USA, [2]Department of Astrophysical and Planetary Sciences, University of Colorado Boulder, Boulder, Colorado, USA, [3]Department of Physics, Imperial College London, London, UK, [4]Department of Physics, University of Colorado Boulder, Boulder, Colorado, USA, [5]NASA Goddard Space Flight Center, Greenbelt, Maryland, USA, [6]Southwest Research Institute, San Antonio, Texas, USA, [7]Department of Physics, University of New Hampshire, Durham, New Hampshire, USA, [8]Royal Institute of Technology, Stockholm, Sweden, [9]Swedish Institute of Space Physics, Uppsala, Sweden, [10]Department of Earth and Space Sciences, University of California, Los Angeles, California, USA, [11]Space Research Institute, Austrian Academy of Sciences, Graz, Austria

**Key Points:**
- Large-amplitude electrostatic waves are observed in the middle of a Kelvin-Helmholtz vortex
- Waves follow fresh mixing of plasma populations with cold electrons present
- Cold electrons may be needed to promote wave growth

**Correspondence to:**
F. D. Wilder,
frederick.wilder@lasp.colorado.edu

**Citation:**
Wilder, F. D., et al. (2016), Observations of large-amplitude, parallel, electrostatic waves associated with the Kelvin-Helmholtz instability by the magnetospheric multiscale mission, *Geophys. Res. Lett.*, *43*, 8859–8866, doi:10.1002/2016GL070404.

Received 11 JUL 2016
Accepted 10 AUG 2016
Accepted article online 12 AUG 2016
Published online 3 SEP 2016



**Abstract** On 8 September 2015, the four Magnetospheric Multiscale spacecraft encountered a Kelvin-Helmholtz unstable magnetopause near the dusk flank. The spacecraft observed periodic compressed current sheets, between which the plasma was turbulent. We present observations of large-amplitude (up to 100 mV/m) oscillations in the electric field. Because these oscillations are purely parallel to the background magnetic field, electrostatic, and below the ion plasma frequency, they are likely to be ion acoustic-like waves. These waves are observed in a turbulent plasma where multiple particle populations are intermittently mixed, including cold electrons with energies less than 10 eV. Stability analysis suggests a cold electron component is necessary for wave growth.

## 1. Introduction

In addition to magnetic reconnection at the dayside subsolar point [*Dungey*, 1961], the Kelvin-Helmholtz instability (KHI) on the flank magnetopause is thought to transfer mass and momentum from the solar wind to the Earth's magnetosphere [*Axford and Hines*, 1961; *Sckopke et al.*, 1981; *Nykyri and Otto*, 2001; *Nakamura and Daughton*, 2014; *Kavosi and Raeder*, 2015]. The KHI, which can form in response to a flow shear across the low-latitude boundary layer (LLBL) on the magnetospheric flanks, manifests as surface waves that propagate along the flow shear direction, and as the instability becomes nonlinear, the waves roll up and form vortices. In the presence of a magnetic field, as these vortices develop, compressed current sheets form in the regions of converging flow, with magnetic field reversals in the boundary layer normal direction [*Nakamura et al.*, 2013]. Recent simulations have suggested that magnetic reconnection can occur on these compressed current sheets, providing another mechanism whereby plasma can be transported across the boundary layer [*Nakamura et al.*, 2013]. Simulations have also shown turbulent cascades down to scales as low as the electron skin depth in KHI vortices [e.g., *Nakamura and Daughton*, 2014].

In March 2015, the four-satellite Magnetospheric Multiscale (MMS) mission was launched to study the kinetic physics of magnetic reconnection [*Burch et al.*, 2015, 2016]. MMS has an eccentric orbit with an apogee designed to skim the magnetopause, which makes it ideal for studying boundary layer phenomena such as the KHI. On 8 September 2015, the MMS constellation encountered the postnoon flank magnetopause during a prolonged period of surface wave activity in the LLBL. Magnetic field, bulk velocity, and density measurements from the inner boundary layer (observed between 09:45:12 and 09:45:59 UT) and the magnetosheath plasma depletion layer (11:27:40–11:28:40 UT), when applied to the linear KHI instability growth theory [e.g., *Chandrasekhar*, 1961], showed positive growth rates for propagation angles within 16° of the direction along the boundary layer. Additionally, periodic current sheets similar to those predicted by *Nakamura et al.* [2013] were observed, approximately half exhibiting magnetic reconnection signatures [*Eriksson et al.*, 2016].

Because simulations suggest that the Kelvin-Helmholtz vortices may contain turbulent plasma due to secondary instabilities, various wave modes can play a role in mediating the energetics and dynamics of the plasma [e.g., *Ergun et al*., 2014a; *Stawarz et al*., 2015]. In this letter, we present one such example observed by MMS on 8 September 2015: large-amplitude ion acoustic-like waves in a region of fluctuating magnetic field. These waves exist in a regime where the ion temperature is greater than the electron temperature, which is usually unfavorable to ion acoustic wave growth [*Kindel and Kennel*, 1971]. We use data from the electric field double probes (EDPs) [*Ergun et al*., 2014b; *Lindqvist et al*., 2014] to investigate the frequency characteristics of the waves, as well as estimate their propagation speed. Ion and electron pitch angle distributions from the fast plasma instrument (FPI) [*Pollock et al*., 2016] when the waves were observed are also shown and demonstrate a fresh mixing of populations. Finally, the electrostatic dispersion relation for reduced parallel electron and ion distributions is analyzed to determine which populations contribute to the wave growth. It is shown that the cold magnetospheric electron population can enable the instability, suggesting that knowledge of this population is important for understanding magnetopause waves.

## 2. Event Overview and Waveform Example

Figure 1 shows the crossing by MMS1 of two periodic vortex-induced current sheets during the 8 September 2015 Kelvin-Helmholtz event. Particle spectrograms and moments were obtained from FPI. The magnetic field data are shown in geocentric solar ecliptic (GSE) coordinates, and the electric field is shown in magnetic field-aligned coordinates (FACs), which is defined as follows: Z is parallel to the background magnetic field ($\mathbf{B}_0$) and is marked with the subscript, "||", *X* is perpendicular to $\mathbf{B}_0$ and in the spacecraft spin plane (P1), and *Y* completes the right-handed system (P2). The electric field was measured at 8192 samples per second. Fluctuations in $|\delta\mathbf{B}|$ with a 10 s running average removed are also shown.

At the beginning of the interval shown in Figure 1, the spacecraft observes plasma with an ion temperature of 1 keV. From the spectrograms, there is a mix of magnetosheath-like ions centered at 1 keV and a lower density population of magnetospheric ions with energies greater than 10 keV. The dawn-dusk component of the magnetic field, $B_Y$, turns increasingly positive during this period until 10:20:57 UT, when it sharply reverses direction. This reversal in $B_Y$ is marked by two vertical dashed lines and is associated with a compressed vortex-induced current sheet as described by *Nakamura et al*. [2013]. After crossing the current sheet, the spacecraft observes magnetosheath ions centered at a few hundred eV and an ion temperature approaching 100 eV. Later, at 10:22:03 UT, the spacecraft observes a second current sheet crossing.

Between the current sheets, $B_Y$ slowly increases from negative to positive, and the ion temperature gradually grows from its magnetosheath value of 100 eV to its magnetospheric value exceeding 1 keV. Additionally, as $B_Y$ crossed zero, the spacecraft observed a lower density magnetospheric ion population with energies exceeding 10 keV in addition to the magnetosheath ions, as seen in the FPI ion spectrograms. Although it is unclear from the event how rolled up the KHI waves are, in the remainder of the study, the region between the compressed current sheets will be referred to as the "vortex" region. The magnetic field fluctuations, $|\delta\mathbf{B}|$, can also provide information on the characteristics of the vortex region. The largest values of $|\delta\mathbf{B}|$ occur near the two $B_Y$ reversals; however, between 10:21:06 and 10:21:48 UT (shown by the vertical dotted lines), there are significant fluctuations in $|\delta\mathbf{B}|$, ranging from 5 to 30 nT. These fluctuations are typically observed in the vortex regions on this day and are largely associated with the magnetic field components perpendicular to the background and therefore should lead to intermittent field-aligned currents. *Eriksson et al.* [2016] suggested that the KH waves were propagating tailward between 200 and 300 km/s, and since these $|\delta\mathbf{B}|$ fluctuations often last for ~1–3 s, this would correspond to current sheets with a thickness of a few hundred kilometers.

During the interval shown in Figure 1, there are two enhancements in the parallel electric field, $E_{||}$. One is near the first $B_Y$ reversal and is spiky in nature and manifests in the electric field spectrum as a broadband pulse. These types of spikes are fairly rare, seen on 15 of the 42 vortex-induced current sheets we examined, and are never seen on more than one spacecraft at a time. They are likely associated with the dynamics of the current sheet and will not be discussed further at this time. The second enhancement observed consists of large-amplitude oscillations near the point in the vortex interval where $B_Y$ crosses zero and the spacecraft begins to observe a mix of magnetosheath and magnetospheric ions. Similar wave trains were seen at this time on all four MMS spacecraft (not shown).

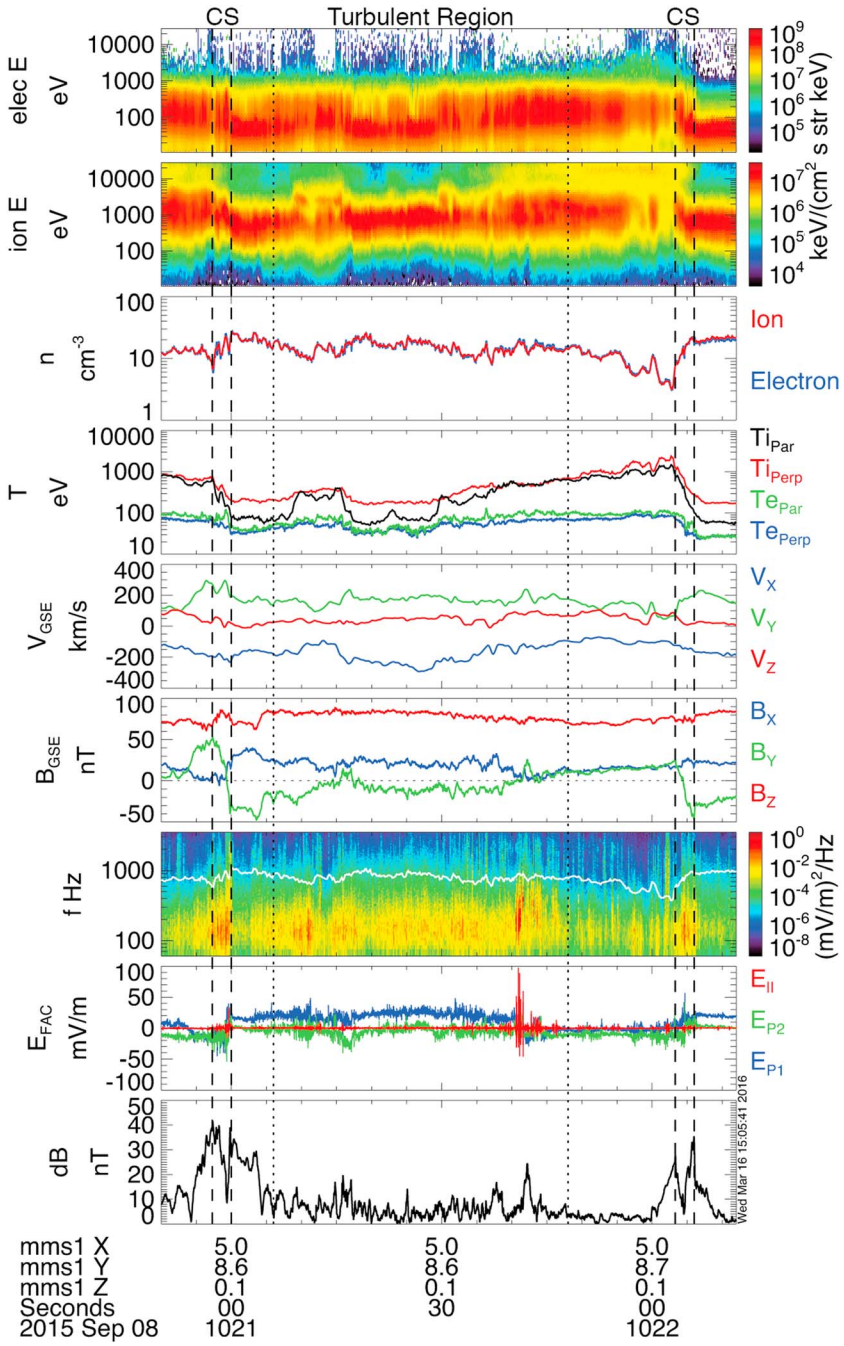


**Figure 1.** Overview example of a single period of KHI oscillations on 8 September 2015. From top to bottom, electron and ion omnidirectional energy spectra, electron and ion number density, electron and ion temperature, ion bulk velocity in GSE, magnetic field vector in GSE, electric field power spectral density (EPSD) in $(mV/m)^2/Hz$, the electric field in FAC, and total magnetic field fluctuations once a 10 s running average is removed. The white line on the spectrum is the ion plasma frequency, the dashed vertical black lines indicate crossings of the vortex-induced current sheets, and the dotted vertical lines indicate the interval with turbulent fluctuations in the magnetic field.

Figure 2 shows a time series of plasma temperature, magnetic field, electric and magnetic field power spectral density, and the electric field in FAC for the wave trains near the $B_Y$ reversal shown in Figure 1. The oscillations are purely electrostatic and only occur in $E_{||}$. Additionally, their spectrum falls between approximately 100 Hz and the ion plasma frequency $\left(f_{pi} = (1/2\pi)\sqrt{(n_i q_e^2)/(m_i \epsilon_0)}\right)$, shown by a white line. Similar waves, although not always as large in amplitude, are seen throughout the vortex portions of the 10:00–11:30 UT

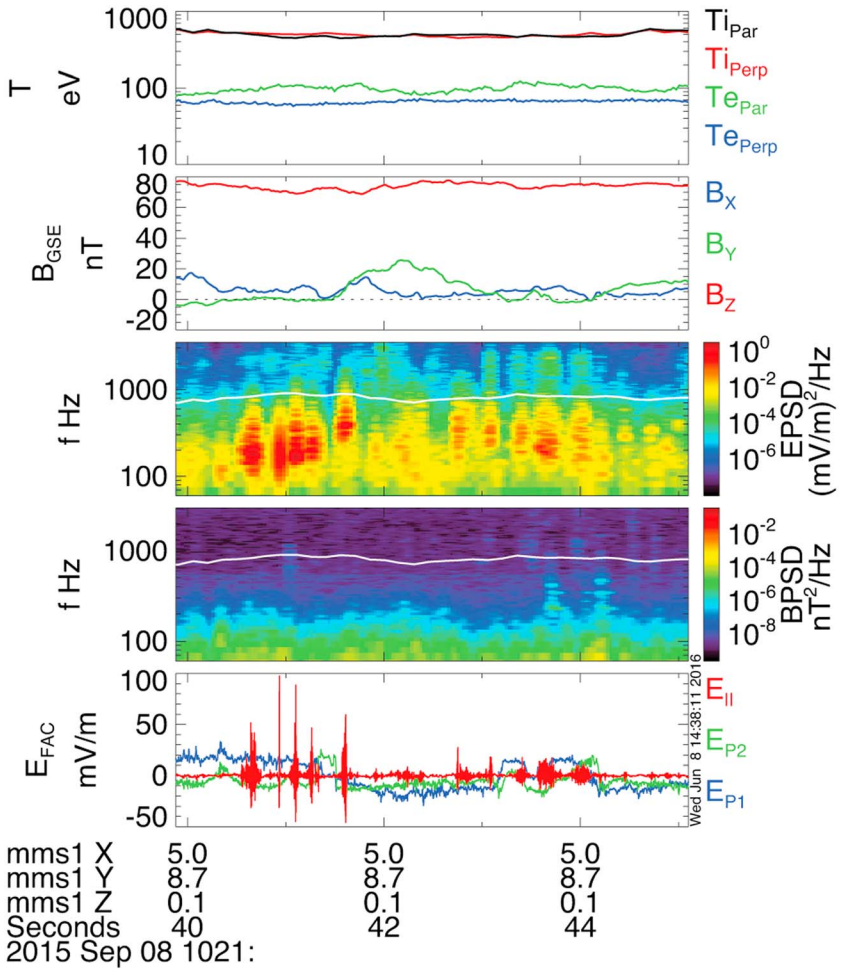


**Figure 2.** Zoom on the large-amplitude parallel electric field oscillations. From top to bottom, ion and electron temperature, magnetic field in GSE, EPSD, magnetic field power spectral density (BPSD), and the electric field in FAC.

Kelvin-Helmholtz interval. Because the oscillations are parallel, electrostatic and below $f_{pi}$, they may be ion acoustic waves [*Kindel and Kennel*, 1971].

One striking characteristic of these waves is that the ion temperature is approximately 6 times greater than the electron temperature. Conditions where $T_i > T_e$ are generally considered unfavorable for ion acoustic waves, since they can experience ion Landau damping. Despite this, the presence of an electron drift, as well as flow shears and field-aligned currents, can still allow the growth of these wave modes [*Kindel and Kennel*, 1971; *Gavrishchaka et al*., 1996]. Additionally, *Ergun et al*. [2016a] suggested that the presence of cold plasma at the magnetopause could also lead to large-amplitude oscillations in the parallel electric field. Therefore, the particle distributions, and not just the moments, must be examined to determine what waves can grow in the Kelvin-Helmholtz instability.

## 3. Particle Distributions

One advantage of MMS is the high resolution at which FPI provides particle distributions—30 ms cadence for electrons and 150 ms for ions [*Pollock et al*., 2016]. Figure 3a shows cuts of the ion pitch angle distribution in the parallel and antiparallel directions between 10:20:37 and 10:21:42 UT. These distributions are in the bulk flow frame. A striking feature of the parallel ions is a dispersive signature that begins with 2–4 keV ions and ends with a shoulder on the distribution centered at a few hundred eV. This dispersion of ions from higher to lower energy suggests an injection from below, possibly from a localized reconnection event, with the faster ions reaching the detector first. This ion shoulder leads to larger parallel temperature moments for the ions

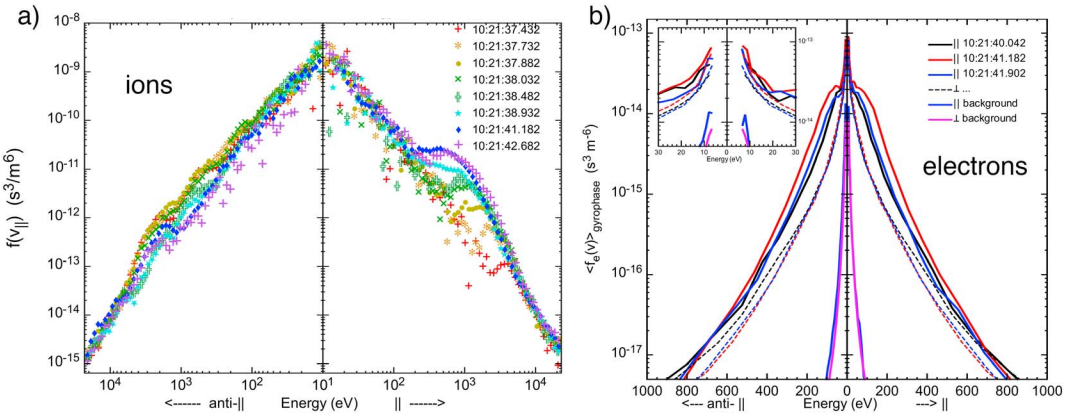


**Figure 3.** (a) Cuts of the observed ion distribution for 0 and 180° pitch angles at several times. (b) Cuts of the observed electron distribution for 0, 180, and 90° pitch angles at three times.

(~500 eV) even though the core of the distribution has $T_{||}$ closer to 40 eV. This illustrates the difficulty in using moments to determine ion acoustic wave stability in this region.

The question remains about whether or not the ion distribution is stable, and a possible cause of the waves observed in Figures 1 and 2. Characterizing the electron population is therefore also important. Figure 3b shows parallel and perpendicular cuts of electrons corrected for background and spacecraft potential at 3 times between 10:20:40 and 10:20:42, as well as the modeled background electrons. The background model is an empirical model of secondary and photoelectrons generated from solar EUV hitting the dual electron spectrometer (DES) instrument surfaces. As opposed to spacecraft photoelectrons, the spacecraft potential does not affect these electrons as they are generated internally within DES. They are similar to a population observed on the Cluster PEACE instrument [*Szita et al.*, 2001]. The detailed angular distribution of these background photoelectrons were measured during MMS commissioning and a running average of their contribution to the measured phase space density were removed from the data shown in Figure 3 [*Pollock et al.*, 2016]. Because the spacecraft potential magnitude is low (~3–4 V), significant spacecraft photoelectron contamination is not expected.

From Figure 3b, there appear to be two electron populations. The first is a sheath-like population with a temperature around 80 eV, and the second is a cold core population. The inlay shows a zoomed in cut of the cold core population, as well as the background model. The cold electron population is an order of magnitude above the background electron signal and appears throughout much of the turbulent region of the Kelvin-Helmholtz vortex. Because of the significant phase space density above the background, and the fact that they, unlike the background, are isotropic, these cold electrons are likely to be real, although the detailed structure below ~10 eV must be approximated using a model. *Ergun et al.* [2016a] suggested that cold electrons were necessary to grow large-amplitude, parallel electrostatic waves near the electron diffusion region on the magnetospheric side separatrix. They observed cold ions but were unable to directly measure the cold electron core.

## 4. Stability Analysis

The particle observations in the present study suggest the mixing of several magnetospheric and magnetosheath populations through intermittent injections associated with the turbulent region of the KH instability. To determine how these populations can provide the free energy needed to grow the waves, the reduced distribution functions, $F_e(v_{||})$ and $F_i(v_{||})$, were calculated for the electrons and ions, respectively, by integrating the distributions over particle velocities perpendicular to $\mathbf{B}_0$. Figures 4a and 4b show $F_e(v_{||})$ and $F_i(v_{||})$, respectively. For $F_e(v_{||})$, the measured distribution at 10:21:41.077 UT is given in blue, where the 3-D distribution for energies below the lowest measured energy (10.935 eV) are interpolated to a value at zero energy equal to the average measured flux at 10.935 eV. For the ions, there is a core population with $T_{||}$ ~ 40 eV, and a shoulder with a center velocity of ~300 km/s. This shoulder is the injected magnetospheric ion population shown in Figure 3a.

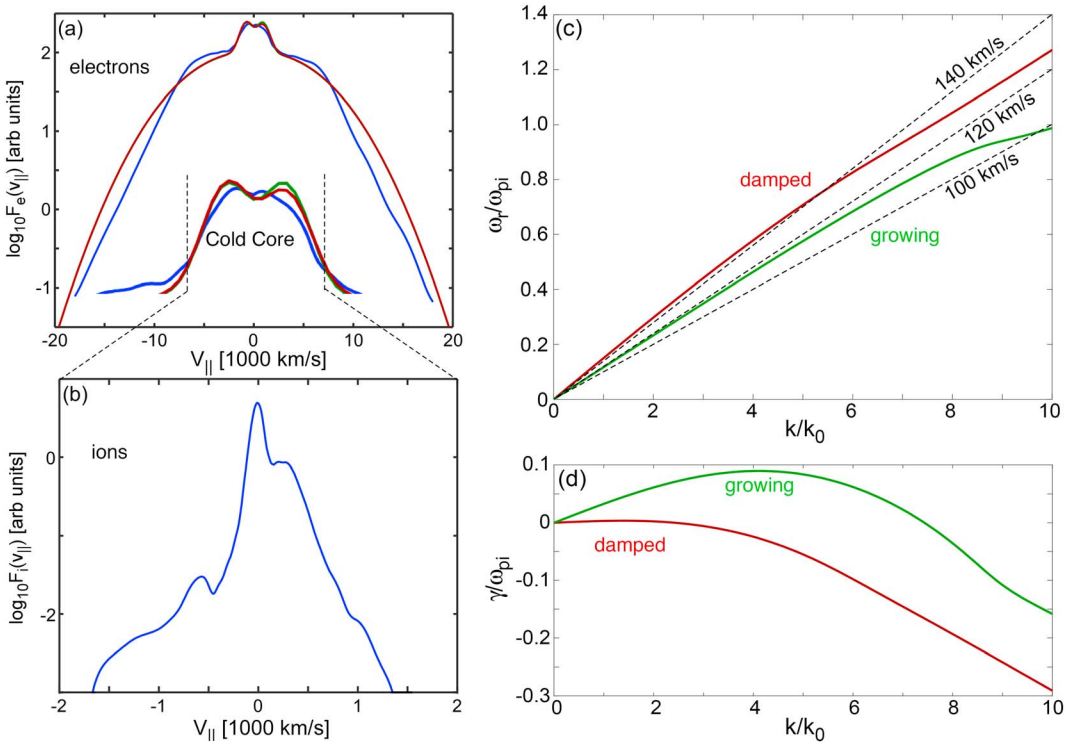


**Figure 4.** (a) The measured (blue) and modeled (red and green) reduced electron distributions, $F_e(v_{||})$, including a zoom on the cold core between −2000 and 2000 km/s. (b) The measured reduced ion distribution function, $F_i(v_{||})$. (c) The real frequency, $\omega_r$, versus $k$ for damped and growing modes. (d) The growth rate $\Upsilon$ versus $k$ for damped and growing modes. Frequency is normalized to $\omega_{pi}$ and wave number is normalized to $k_0 = \omega_{pi}/(10^3 \text{km/s})$.

To evaluate the stability of these distributions, we use the fact that the dielectric tensor, $\epsilon(\omega, \boldsymbol{k})$, can be represented by the sum of susceptibilities, $\chi(\omega,\mathbf{k})$, for the various electron ($e$) and ion ($i$) populations, as given in equation (1).

$$\epsilon(\omega,\ \boldsymbol{k}) = 1 + \sum_l \chi_e^l(\omega, \boldsymbol{k}) + \sum_m \chi_i^m(\omega, \boldsymbol{k}) \tag{1}$$

The susceptibility for a single dimension (parallel to $\mathbf{B}_0$) from *Friede and Conte* [1961] can then be determined using Z functions to define the susceptibilities for a combination of Maxwellian distributions. For the ions, in order to capture the shoulder, the distribution is incorporated directly into the dispersion solver by representing it as a sum of multiple narrow Maxwellians in order for the standard Landau prescription to be well-defined for weakly damped modes. For the electrons, we use two slightly different model distributions, one which leads to damping of electrostatic waves and one which leads to wave growth, as shown in Figure 4a in red and green, respectively. The model distributions consist of four Maxwellian components: two hot and two cold. The hot populations each have a temperature of 100 eV and together comprising 96% of the total electron density. To mimic the broad shoulders of the observed distribution, they are given oppositely directed mean drift velocities corresponding to that of a 5 eV electron. In the unstable model distribution the two cold populations each comprise 2% of the total electron density; both have a temperature of 2 eV; and their mean drifts respectively correspond to energies of 1.25 eV (toward the left) and 1.5 eV (toward the right). The stable distribution differs only in that the temperature of the rightward cold population has been increased to 2.25 eV. We note that the double-hump feature of the model electron distribution involves electrons that cannot be directly observed due to their low energy. However, this notch-like feature in the unstable distribution is not inconsistent with the observations and can be viewed as the result of introducing a drifting cold beam to the population.

Performing this stability analysis yields several important results. First, while the ion shoulder may appear unstable, the dispersion solver reveals that any wave mode resonant with this shoulder is damped by the broad electron distribution. Since this dispersive ion feature ends approximately 2 s before the waves are

observed, it is unlikely to be the source of the wave growth. Second, the main way to introduce wave growth using the distributions was to generate a notch in the cold electrons. Figures 4c and 4d show the results of the dispersion solver for both damped and growing solutions, shown by red and green lines, respectively. The growing waves (green) are produced by enhancing the phase space density of the forward drifting parallel electrons. The phase speed of the stable waves is between 100 and 120 km/s, which is fairly close to the ion acoustic speed using the temperature of the ~40 keV core (~130 km/s). The frequency of maximum growth is between 0.3 and 0.5 $f_{pi}$, which corresponds to a few hundred hertz in this case.

## 5. Summary and Conclusion

This letter presented first observations of large-amplitude, parallel, electrostatic waves associated with the KHI on the dusk flank magnetopause by the MMS mission. Additionally, they had a frequency below $f_{pi}$, suggesting they may be ion acoustic waves. It was shown that the ratio between electron and ion temperatures was less than one, which by the dispersion relation from *Kindel and Kennel* [1971] leads to damped ion acoustic waves. However, analysis of the distributions showed an ion shoulder in the parallel direction that resulted from a dispersive burst, which led to a larger apparent ion $T_{||}$ when calculating the moments of the distribution. The ion core temperature was lower than the electron temperature. Additionally, a cold electron population that was significantly above the spacecraft background was found.

Stability analysis was performed by solving the dispersion relation (1), with several important results. First, any instability resulting from the ion shoulder is damped by the main electron distribution. Second, introducing a notch in the electron distribution by having multiple drifting populations in the cold electron core was enough to generate wave growth. This suggests the cold component of the electrons may be playing a role in wave growth. Third, the ions do enhance the growth rate of the waves associated with the drifting cold electrons, suggesting that the ions can also play a minor role in the instability.

The MMS mission has observed multiple instances of large-amplitude parallel electric field structures on the magnetopause. These can include double-layer-like structures that are thought to be a signature of the detangling of flux ropes, or "secondary reconnection" [*Ergun et al*., 2016b]. Electrostatic parallel electric field structures can also be related to the dissipation of turbulence in space plasmas [e.g., *Ergun et al*., 2016a; *Stawarz et al*., 2015], which likely includes the magnetopause. Finally, they can also include large-amplitude electrostatic waves near the electron diffusion region at the subsolar magnetopause, such as those observed by *Ergun et al*. [2016a]. *Ergun et al*. [2016a] confirmed the presence of cold ions using both the FPI instrument and the presence of wake signatures in the axial electric field instruments and inferred that cold electrons must also be present. They showed that a drifting cold electron population mixing with the magnetosheath electrons led to a parallel electrostatic wave mode on the magnetospheric side that was an acoustic response in the frame of the sheath electrons, and a Langmuir response in the frame of the cold electrons. They also suggested that other wave modes could grow as a result of the mixing of cold and hot particle populations, including ion acoustic waves. These types of waves can be important for two reasons—first, in the nonlinear phase of the wave growth, the waves could be associated with a net field-aligned potential drop that can accelerate electrons. Second, because they result from the mixing of plasma populations, they could serve as an identifier that a spacecraft is near the reconnection diffusion region.

All of these different parallel electric field structures are directly related to understanding magnetic reconnection at the subsolar magnetopause, and knowledge of the cold magnetospheric population is important for differentiating between them. Because the Kelvin-Helmholtz instability can also lead to the mixing of plasma populations, it is likely that instabilities associated with magnetospheric cold electrons may also be important on the magnetospheric flanks as well. Because of their orbit and the fact that they provide high-resolution 3-D electric and magnetic fields, the MMS spacecraft are ideal for future studies on the types of wave modes that can grow as a result of the mixing of magnetosheath and magnetospheric populations, as well as their relation to other magnetopause phenomena.

**Acknowledgments**
This work was funded by the NASA MMS project. S.J.S. thanks the Leverhulme Trust for the award of a research fellowship. We thank the MMS search coil magnetometer team for providing burst data and comments on our analyses. Level 2 spacecraft data are available via the MMS Science Data Center (https://lasp.colorado.edu/mms/sdc/public/).

## References

Axford, W., and C. Hines (1961), A unifying theory of high-latitude geophysical phenomena and geomagnetic storms, *Can. J. Phys.*, *39*, 1433.
Burch, J. L., T. E. Moore, R. B. Torbert, and B. L. Giles (2015), Magnetospheric Multiscale overview and science objectives, *Space Sci. Rev.*, Online First, doi:10.1007/s11214-015-0164-9.

Burch, J. L., et al. (2016), Electron scale measurements of magnetic reconnection in space, *Science*, doi:10.1126/science.aaf2939.
Chandrasekhar, S. (1961), *Hydrodynamic and Hydromagnetic Stability*, Oxford Univ. Press, New York.
Dungey, J. W. (1961), Interplanetary magnetic field and the auroral zones, *Phys. Rev. Lett.*, *6*, 47–48.
Ergun, R. E., K. A. Goodrich, J. E. Stawarz, L. Andersson, and V. Angelopoulos (2014a), Large-amplitude electric fields associated with bursty bulk flow braking in the Earth's plasma sheet, *J. Geophys. Res. Space Physics*, *120*, 1832–1844, doi:10.1002/2014JA020165.
Ergun, R. E., et al. (2014b), The axial double probe and fields signal processing for the MMS mission, *Space Sci. Rev.*, doi:10.1007/s11214-014-0115-x.
Ergun, R. E., et al. (2016a), Magnetospheric Multiscale observations of large-amplitude, parallel, electrostatic waves associated with magnetic reconnection at the magnetopause, *Geophys. Res. Lett.*, *43*, 5626–5634, doi:10.1002/2016GL068992.
Ergun, R. E., et al. (2016b), Magnetospheric multiscale satellites observations of parallel electric fields associated with magnetic reconnection, *Phys. Rev. Lett.*, *116*, 235,102, doi:10.1103/PhysRevLett.116.235102.
Eriksson, S., et al. (2016), Magnetospheric Multiscale observations of magnetic reconnection associated with Kelvin-Helmholtz waves, *Geophys. Res. Lett.*, *43*, 5606–5615, doi:10.1002/2016GL068783.
Fried, B. D., and S. D. Conte (1961), *The Plasma Dispersion Function*, Academic Press, San Diego, Calif.
Gavrishchaka, V., M. E. Koepke, and G. Ganguli (1996), Dispersive properties of a magnetized plasma with a field-aligned drift and inhomogeneous transverse flow, *Phys. Plasmas*, *3*(8), doi:10.1063/1.871656.
Kavosi, S., and J. Raeder (2015), Ubiquity of Kelvin-Helmholtz waves at Earth's magnetopause, *Nat. Commun.*, *6*, 7019, doi:10.1038/ncomms8019.
Kindel, J. M., and C. F. Kennel (1971), Topside current instabilities, *J. Geophys. Res.*, *76*, 3055, doi:10.1029/JA076i013p03055.
Lindqvist, P.-A., et al. (2014), The spin-plane double probe electric field instrument for MMS, *Space Sci. Rev.*, doi:10.1007/s11214-014-0116-9.
Nakamura, T. K. M., and W. Daughton (2014), Turbulent plasma transport across the Earth's low-latitude boundary layer, *Geophys. Res. Lett.*, *41*, 8704–8712, doi:10.1002/2014GL061952.
Nakamura, T. K. M., W. Daughton, H. Karimabadi, and S. Eriksson (2013), Three-dimensional dynamics of vortex-induced reconnection and comparison with THEMIS observations, *J. Geophys. Res. Space Physics*, *118*, 5742–5757, doi:10.1002/jgra.50547.
Nykyri, K., and A. Otto (2001), Plasma transport at the magnetospheric boundary due to reconnection in Kelvin-Helmholtz vortices, *Geophys. Res. Lett.*, *28*, 3565–3568, doi:10.1029/2001GL013239.
Pollock, C., et al. (2016), Fast plasma investigation for magnetospheric multiscale, *Space Sci. Rev.*, *199*, 331, doi:10.1007/s11214-016-0245-4.
Sckopke, N., G. Paschmann, G. Haerendel, B. U. O. Sonnerup, S. J. Bame, T. G. Forbes, J. E. W. Hones, and C. T. Russell (1981), Structure of the low-latitude boundary layer, *J. Geophys. Res.*, *86*, 2099–2110, doi:10.1029/JA086iA04p02099.
Stawarz, J. E., R. E. Ergun, and K. A. Goodrich (2015), Generation of high-frequency electric field activity by turbulence in the Earth's magnetotail, *J. Geophys. Res. Space Physics*, *120*, 1845–1866, doi:10.1002/2014JA020166.
Szita, S., A. N. Fazakerley, P. J. Carter, A. M. James, P. Travnicek, G. Watson, M. Andre, A. Eriksson, and K. Torkar (2001), Cluster PEACE observations of electrons of spacecraft origin, *Ann. Geophys.*, *19*, 10, doi:10.5194/angeo-19-1721-2001.